Heparin Binding Site, Conformational Change, and Activation of Antithrombin†

Dyfed Ll. Evans,*,‡ Craig J. Marshall,§ Peter B. Christey,‡ and Robin W. Carrell‡

Department of Haematology, University of Cambridge, MRC Centre, Hill's Road, Cambridge CB2 2QH, U.K., and Department of Biochemistry, University of Otago, Dunedin, New Zealand

Received April 22, 1992; Revised Manuscript Received September 10, 1992

ABSTRACT: Alignment of the heparin-activated serpins indicates the presence of two binding sites for heparin: a small high-affinity site on the D-helix corresponding in size to the minimal pentasaccharide heparin, and a longer contiguous low-affinity site extending to the reactive center pole of the molecule. Studies of the complexing of antithrombin and its variants with heparin fractions and with reactive center loop peptides including intermolecular loop–sheet polymers all support a 3-fold mechanism for the heparin activation of antithrombin. Binding to the pentasaccharide site induces a conformational change as measured by circular dichroism. Accompanying this, the reactive center becomes more accessible to proteolytic cleavage and there is a 100-fold increase in the k_{ass} for factor Xa but only a 10-fold increase for thrombin, to 6.4×10^4 M^{-1} s^{-1}. To obtain a 100-fold increase in the k_{ass} for thrombin requires in addition a 4:1 molar ratio of disaccharide to neutralize the charge on the extended low-affinity site. Full activation requires longer heparin chains in order to stabilize the ternary complex between antithrombin and thrombin. Thus, addition of low-affinity but high molecular weight heparin in conjunction with pentasaccharide gives an overall k_{ass} of 2.7×10^6 M^{-1} s^{-1}, close to that of maximal heparin activation.

The serpins are a superfamily of serine protease inhibitors (Huber & Carrell, 1989) that share a tightly conserved single tertiary structure, the best studied members being those present in human plasma. A minority of serpins require activation by polysulfated oligosaccharides before they become effective inhibitors; notable examples are antithrombin (antithrombin III or ATIII),[1] heparin cofactor II (HCII), protease nexin I (PNI), plasminogen activator inhibitor 1 (PAI–1), and protein C inhibitor (Kuhn et al., 1990). Collectively, these are known as heparin-activatable serpins though the term is misleading as heparin is a heterogeneous animal extract containing a mixture of glycosaminoglycans, and for example, heparin cofactor II is most effectively activated by dermatan sulfate rather than heparin (Tollefsen et al., 1986). Nevertheless, it shares a homologous binding site with antithrombin and PNI (Borg et al., 1988; Carrell et al., 1987; Evans et al., 1990). We summarize evidence here for this common site, but most of our studies relate to antithrombin and the observations that this can be activated differentially by various heparin fractions (Holmer et al., 1981; Oosta et al., 1981; Ellis et al., 1986).

Heterogeneous heparin can be fractionated on an antithrombin–Sepharose column (Höök et al., 1976; Lam et al., 1976), both before and after hydrolysis, into fractions of varying molecular weights, some with high and some with low affinity for ATIII. In particular, the smallest fraction with high affinity has been shown to be a well-defined pentasaccharide with four (Choay et al., 1989) essential sulfates; this pentasaccharide effectively activates antithrombin as an inhibitor of the clotting protease Xa but not as an inhibitor of thrombin. Full activation for thrombin inhibition requires a high-affinity fraction of greater than 18-mer size (Peterson & Blackburn 1987; Ellis et al., 1986)—this high molecular weight fraction will be referred to hereafter as high-affinity heparin. The heparin fractions that bind with low affinity to antithrombin (Lam et al., 1976) have by themselves little effect on its activation but are important experimentally and will subsequently be referred to here as low-affinity heparin.

Recently, we have investigated the properties of variants of human antithrombin with abnormal heparin affinity (Owen et al., 1987; Brennan et al., 1988; Gandrille et al., 1990) and have also studied the heparin binding properties of novel conformational forms of antithrombin (Carrell et al., 1991). We have shown that the serpins have a mobile reactive center which can move in and out of the A-sheet of the molecule giving this sheet an alternative five- or six-stranded structure. Cleavage of the reactive center gives the R form (Löbermann et al., 1984) in which the peptide loop is reincorporated into the sheet as the middle s4A strand. It is likely that the reactive center in the native inhibitor is in the partially reincorporated "canonical" structure necessary for inhibition. Two further conformations can be induced in antithrombin; a latent L-form (Carrell et al., 1991; Mottonen et al., 1992), where the molecule has the physical properties of the R form but has an intact reactive center loop; and the binary complex form in which synthetic peptide homologues of the reactive center loop are annealed into the A-sheet (Schulze et al., 1990) and the loop probably takes the helical conformation of that in ovalbumin (Stein et al., 1990). Furthermore, antithrombin (Evans, 1991), as with inhibitory serpins (Lomas et al., 1992; Mast et al., 1992), can undergo polymerization on prolonged incubation by a loop–sheet mechanism in which the reactive center loop of one molecule inserts into the A-sheet of another.

In this paper, we report additional studies which together with previous work indicate a 3-fold action of heparin on antithrombin: binding of the pentasaccharide takes place at a specific high-affinity site and is accompanied by a conformational change; a second contiguous low-affinity site allows

† This work was supported by the Medical Research Council and the Wellcome Trust.

‡ University of Cambridge.

§ University of Otago.

[1] Abbreviations: ATIII, antithrombin III and antithrombin; PNI, protease nexin I; HCII, heparin cofactor II; PAI-1, plasminogen activator inhibitor-1; SDS, sodium dodecyl sulfate; PAGE, polyacrylamide gel electrophoresis; HPLC, high-pressure liquid chromatography; ΔUA, dermatan sulfate derived disaccharide ΔUA→GalNac-4S,6S; GdmCl, guanidinium chloride; PVDF, poly(vinyl difluoride); CD, circular dichroism.

0006-2960/92/0431-12629$03.00/0

charge neutralization of the reactive center pole of the molecule; and high molecular weight heparin provides a bridge between protease and inhibitor to give the stabilized ternary complex.

EXPERIMENTAL PROCEDURES

Materials. Human neutrophil elastase was a gift from Dr. P. M. George (Department of Pathology, Christchurch Hospital, New Zealand), plasmin was a gift from Dr. P. A. Pemberton (Immunology Division, Children's Hospital, Boston, MA), human α-thrombin was a gift from Dr. J.-M. Freyssinet (Institut d'Hématologie et d'Immunologie, Facilité de Médicine, Strasbourg, France), *Pseudomonas aeruginosa* elastase was a gift from Dr. K. Morihara (Kyoto research laboratories, Tokyo, Japan), and the heparin pentasaccharide corresponding to the minimal sequence of heparin necessary for antithrombin III activation (Torri et al., 1985; Choay, 1989) was a gift from the Institute Choay, Paris. Porcine mucosal heparin, low molecule weight heparins, and additional proteases were from Sigma Chemical Co. The disaccharide ΔUA→GalNac-4S,6S was obtained from Grampian Enzymes, Arthrath, Scotland. S2251 was obtained from KabiVitrum Ltd., and succinyl-alanyl-alanyl-alanyl-*p*-nitroanilide was from Sigma, while all other substrates were obtained from Boehringer Mannheim. The Mono Q column, Sepharose Cl 6B, and S-Sepharose fast-flow were obtained from Pharmacia. All other reagents and chemicals were from Sigma.

Computational Methods. Blocked alignments of the serpins were prepared using the Needleman–Wunsch algorithm, with modification to penalize for introducing gaps into regions of defined secondary structure (Lesk et al., 1984).

Antithrombin Purification. Wild-type antithrombin was isolated by the method of McKay (1981), with further purification to homogeneity, by size exclusion on a 1.2-m-high Sephacryl S-200 column. The antithrombin variant, Geneva (129Arg → Gln) (Gandrille et al., 1990), was kindly provided in isolated form by D. Bruce (University of Cambridge, Department of Hæmatology, U.K.). The variant Rouen I (47Arg → His) (Owen et al., 1987) was isolated from the plasma of a patient with normal levels of antithrombin and normal progressive activity but only 61% heparin cofactor activity. Antithrombin Toyama (47Arg → Cys) (Koide et al., 1984) was also isolated from the plasma of a patient with normal antithrombin antigenic levels and normal progressive activity but only 68% heparin cofactor activity. These variants were isolated to homogeneity, as described previously (Owen et al., 1987; Koide et al., 1984), by heparin affinity chromatography.

Heparin Fractionation. Heparin was fractionated as described previously (Evans et al., 1991).

Formation of Latent (L), Binary Complexed (BC), and Polymerized ATIII. Latent ATIII was produced by treatment of 1 mg/mL antithrombin with 0.9 M GdmCl at 4 °C overnight in 50 mM Tris, 50 mM NaCl, pH 7.6, before dialysis for 48 h at 4 °C into 50 mM phosphate, 10 mM NaCl, pH 7.2, as described previously (Carrell et al., 1991). Binary complexes of ATIII with the peptides A (Ac-Ser-Glu-Ala-Ala-Ala-Ser-Thr-Ala-Val-Val-Ile-Ala-Gly-OH (corresponding to residues 370–382 in ATIII) and C (Ac-Ser-Glu-Ala-Ala-Ala-Ser-Thr-Ala-Val-OH (corresponding to residues 370–378 in ATIII)) were produced by incubation of ATIII and peptide at 1:100 molar ratios, as described previously (Carrell et al., 1991; Lomas et al., 1992), in either the presence or absence of heparin. Kinetics of binary complex formation were determined by loss of thrombin inhibitory activity on the basis of the reaction

$$S + P_t \xrightarrow{k_{obs}} BC$$

where S is the serpin, P_t the peptide, and BC the resultant binary complex. Under pseudo-first-order conditions, with a vast excess of peptide, the observed association rate k_{obs} is given by

$$k_{obs} = \frac{1}{T_{1/2}[P_t]_0}$$

where $T_{1/2}$ is the half-time of interaction and $[P_t]_0$ is the original peptide concentration. Loop–sheet polymers of ATIII were produced by incubating ATIII in 50 mM sodium phosphate, 50 mM NaCl, pH 7.6, at 65 °C for 6 days in either the presence or absence of pentasaccharide. Polymerization was followed by HPLC analysis on a molecular weight calibrated TSK 2000SW size-exclusion column (Evans, 1991; Lomas et al., 1992): 20-μg samples were loaded at a flow rate of 0.5 mL/min in 50 mM phosphate buffer, pH 7.6. Native ATIII eluted from the column at 13.6 min, while polymer (greater than 200-kDa) eluted from the column at 11.4 min. Measurement of the increase in the first peak gave the rate of polymerization. ATIII polymerization only occurred with intact ATIII and was effectively stopped by cleavage at the reactive center, formation of the L form, or binary complex production. It could also be reversed by incubation with reactive center peptides (Lomas et al., 1992).

Nondissociating PAGE. The method used was that of Goldenberg (1989), except that for running the gel the cathodic buffer used was 3.9 g of glycine, 6.4 g of Tris in 1 L of distilled water, and the anodic buffer was 12.1 g of Tris, 50 mL of 1 M HCl in 1 L of distilled water.

Kinetic Measurements. The protocol was based on that of Beatty et al. (1980). Active site titrations with α-thrombin and trypsin were carried out by the method of Chase and Shaw (1969). These proteases were used to titrate ATIII, which was then used to titrate the other proteases analyzed.

Data were analyzed kinetically under second-order conditions, at equimolar concentrations of protease and inhibitor, where

$$t_{1/2} = \frac{1}{k_{ass}[P]_0}$$

where $[P]_0$ is the initial protease concentration and $t_{1/2}$ is the half-life of the interaction. Controls containing the various heparin fragments were utilized to ensure that heparin had no effect on the rate of substrate hydrolysis. No effects were observed in any of the reaction mixtures.

Reactions were conducted at room temperature in a total volume of 200 μL of 50 mM Tris-HCl, 0.15 M NaCl, 0.1% PEG 6000, 0.1 mg/mL BSA, pH 8.2. To this, chromogenic substrate in 800 μL of assay buffer was added in 250–2000-fold excess, both to prevent further interaction between protease and inhibitor and to facilitate measurement of remaining active protease. The effects of Cl^- ions on the interaction of antithrombin with thrombin in the presence and absence of pentasaccharide were determined as above, but using 20 mM Tris-MOPS, 0.1% PEG 6000 pH 7.4 buffer, with increasing concentrations of $MnCl_2$ from 0 to 2 M.

Proteolytic Cleavages of ATIII. Porcine pancreatic elastase, *P. aeruginosa* elastase, and human neutrophil elastase cleavages of ATIII were conducted at enzyme:inhibitor ratios of 1:170, 1:200, and 1:360 (w/w), respectively in 50 mM Tris-

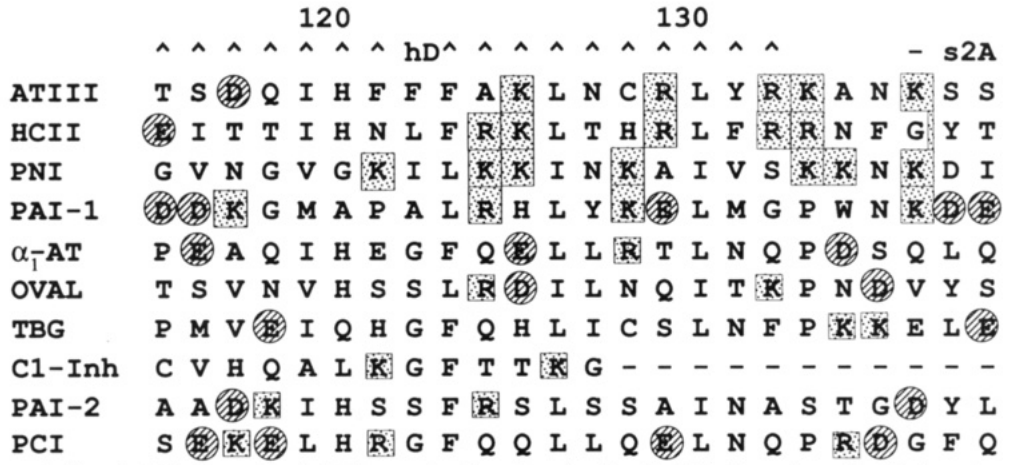

FIGURE 1: Alignment of serpin D-helices: Blocked alignments of serpins, showing the D-helix regions. Positively and negatively charged residues are highlighted and indicate uniquely conserved regions of positive charge on the external face of the D-helices of the heparin-activable members (ATIII, HCII, PNI, and PAI-1). α_1-Antitrypsin secondary structure and ATIII numbering are used. Abbreviations: ATIII, antithrombin III; HCII, heparin cofactor II; PNI, protease nexin I; PAI-1, plasminogen activator inhibitor 1; α_1-AT, α_1-antitrypsin; oval, ovalbumin; TBG, thyroxine binding globulin; C1-inh, C1 inhibitor; PAI-2 plasminogen activator inhibitor 2; PCI, protein C inhibitor.

HCl, 200 mM NaCl, 1 mM $CaCl_2$, 50 mM $ZnCl_2$, pH 7.0, for 2 h at 37 °C. The reactions were terminated by the addition of diisopropyl fluorophosphate to a final concentration of 20 μM.

Cleaved peptide bonds were identified by electrophoresis of the cleaved ATIII on 10–20% SDS–PAGE gels, blotting onto PVDF, and N-terminal sequencing from the blot (Matsudaira, 1987).

Kinetic Analyses of Cleavage Reactions. Samples were removed from the cleavage reactions, with the concentration of active ATIII being measured by thrombin inhibition assay.

Utilizing the property that serpin cleavage is irreversible, the standard substrate reaction mechanism becomes

$$S + E \underset{k_{-1}}{\overset{k_1}{\rightleftharpoons}} ES \xrightarrow{k_2} P + E$$

and the integrated form of the Michaelis–Menten equation is derived (Walker & Schmidt, 1944; Wharton & Szawelski, 1982):

$$V_{max}t = [P] + K_M \ln\left(\frac{[S]_0}{[S]_0 - [P]}\right) \quad (1)$$

which can be reexpressed as

$$\frac{[P]}{t} = V_{max} - \frac{K_M}{t} \ln\left(\frac{[S]_0}{[S]_0 - [P]}\right) \quad (2)$$

where S = substrate, P = product, K_M = Michaelis complex ($=(k_{-1} + k_2)/k_1$), and $V_{max} = k_2[E]_0$ ($[E]_0$ = initial enzyme concentration). Using these equations and substituting the values for [S], [P], and time t, K_M and k_2 can be found.

Heat Stability Assays. One-milliliter samples of ATIII (0.1 mg/mL in 75 mM NaH_2PO_4, 75 mM glycine, 75 mM Tris-HCl, pH 7.5) were heated at 60 °C for 8 h in the presence of 0:1, 0.05:1, 0.5:1, 1:1, and 10:1 molar ratios of heparin to antithrombin, with 100-μL samples being removed at hourly intervals, centrifuged in a microcentrifuge for 15 min, and filtered (0.45-μm pore size filters). The final concentration of ATIII in the supernatant was measured by rocket immunoelectrophoresis (Laurell, 1966).

ATIII Heparin-Affinity Determination. Heparin affinities were determined using 55 mm × 15 mm columns of heterogeneous and high-affinity heparin–Sepharose (produced by cyanogen bromide activation of Sepharose and coupled with 0.75 mg of heparin/mL of gel), attached to a Waters 600E advanced protein purification system. Samples were loaded in 20 mM NaCl, 20 mM Tris-HCl, pH 7.5, at a flow rate of 0.5 mL/min. Elution was achieved by a 1.5-h linear gradient from 20 mM NaCl, 20 mM Tris-HCl, pH 7.5, to 1.0 mM NaCl, 20 mM Tris-HCl, pH 7.5, at a flow rate of 1 mL/min.

Circular Dichroism. Circular dichroism measurements were conducted in 20 mM sodium phosphate, 30 mM NaCl, pH 7.8, at 30 °C in a Jobin-Yvon Dichrographe VI instrument. Spectra were measured in terms of mean residue ellipticity $[\theta]_{MRW}$ in deg·cm^2·dmol^{-1}, using a mean residue weight of 134. Spectra in the near-UV region (260–330 nm) were determined with a 1-cm-path-length cell, while those in the far-UV region (200–260 nm) were determined with a 0.1-cm-path-length cell. Spectra shown are the average of 36 readings (two sets of 18), taken on two separate occasions. In all cases, 1:1 molar ratios of heparin:antithrombin were used.

RESULTS

Heparin Binding Site. Previous studies (Carrell et al., 1987; Huber & Carrell, 1989; Evans et al., 1990) showed that blocked alignments of serpins in the region of the D-helix indicated a unique and well-conserved region of positive charge on the external face of this helix in ATIII, PNI, and HCII. This homology has now been extended by Ehrlich et al. (1991) to include PAI-1 (Figure 1). Projection of these residues onto a model of ATIII indicates a further less-well-conserved region of positive charge extending from the D-helix toward the N-terminus and reactive center poles of each of these serpins (Table I), which was not observed in the heparin binding serpin, protein C inhibitor.

Heparin Activation of ATIII. To dissect the mechanisms involved in the heparin activation of ATIII, a comparison was made of the effects of pentasaccharide and 25-kDa high- and low-affinity heparins on the rates of thrombin, factor Xa, and plasmin inhibition by wild-type ATIII and by the heparin affinity mutants ATIII Rouen I (47Arg → His) and ATIII Geneva (129Arg → Gln).

The charge carried by His47 in ATIII Rouen I can be predicted according to pH; at pH 8.0 the histidine predictably is deprotonated and carries no charge, while at pH 6.0 the histidine is protonated and thus carries a positive charge. A comparison was made of the rate of inhibition at both pH

Table I: Heparin Binding Sites[a] of ATIII, PNI, HCII, and PAI-1

serpin	D-helix high-affinity site	extended binding site
ATIII	Lys125, Arg129, Arg132, Lys133, Lys136, Lys228	Arg46, Arg47, Arg114, Arg235, Lys236, Lys275
HCII	Lys125 (185), Arg129 (189), Arg132 (192), Arg133 (193), Lys228 (288)	Arg47 (107), Arg50 (110), Arg114 (173), Arg124 (184), Lys223 (283), Arg416 (476)
PNI	Lys125 (94), Lys128 (97), Lys133 (102), Lys134 (103), Lys136 (105), Lys227 (196)	Arg97 (66), Lys99 (68), Lys100 (69), Arg90 (59), Lys93 (62), Lys204 (173), Arg227 (196), Lys236 (205), Lys237 (206)
PAI-1	Arg124 (76), Lys128 (80), Lys136 (88), Lys224 (176)	Lys117 (69), Lys152 (104), Arg163 (115), Arg210 (162), Arg235 (187), Arg236 (188), Lys239 (191), Lys325 (277), Arg348 (300), Arg402 (354), Arg409 (361)

[a] Residues indicated were identified as potentially involved in the serpin–heparin interaction. Initial direct sequence homology identified the prime site (Figure 1). A further analysis of each individual serpin identified the more variable extensions of the positively charged site, to the N- and C-termini. The largest secondary site was identified in PNI and the smallest in HCII. These variations help explain the different heparin affinities of each of these inhibitors. Numbering is that of the homologous ATIII sequence, with the actual sequence number in brackets.

Table II: Effect of Heparins on Inhibition Rates of ATIII Mutants[a]

enzyme (human) (final molarity)	substrate (final molarity)	glycosaminoglycan (final molarity)	ATIII (wild), Arg47,129, k_{ass} (M^{-1} s^{-1}) (mean ± SE)	ATIII Rouen I, His47, pH 6.0, k_{ass} (M^{-1} s^{-1}) (mean ± SE)	ATIII Rouen I His47, pH 8.0, k_{ass} (M^{-1} s^{-1}) (mean ± SE)	ATIII Geneva, Gln129, k_{ass} (M^{-1} s^{-1}) (mean ± SE)
α-thrombin (53 nM)	chromozym TH (0.12 mM)		$(5.5 \pm 0.3) \times 10^3$	$(5.4 \pm 0.4) \times 10^3$	$(5.5 \pm 0.2) \times 10^3$	$(4.3 \pm 0.4) \times 10^3$
α-thrombin (53 nM)		pent. (51 nM)	$(6.4 \pm 0.2) \times 10^4$	$(4.3 \pm 0.3) \times 10^4$	$(2.5 \pm 0.3) \times 10^3$	$(3.9 \pm 0.5) \times 10^3$
α-thrombin (20 nM)		25-kDa LA (20 nM)	$(2.2 \pm 0.2) \times 10^4$	$(2.2 \pm 0.2) \times 10^4$	$(2.0 \pm 0.4) \times 10^4$	$(1.2 \pm 0.2) \times 10^4$
α-thrombin (15 nM)		25-kDa HA (15 nM)	$(8.7 \pm 0.5) \times 10^7$	$(4.7 \pm 0.6) \times 10^6$	$(1.9 \pm 0.2) \times 10^4$	$(1.3 \pm 0.2) \times 10^4$
factor Xa (80 nM)	chromozym X (0.69 nM)		$(2.8 \pm 0.2) \times 10^3$	$(2.7 \pm 0.4) \times 10^3$	$(3.0 \pm 0.4) \times 10^3$	$(2.6 \pm 0.3) \times 10^3$
factor Xa (80 nM)		pent. (80 nM)	$(3.7 \pm 0.4) \times 10^5$	$(2.9 \pm 0.4) \times 10^5$	$(2.9 \pm 0.2) \times 10^3$	$(2.7 \pm 0.4) \times 10^3$
factor Xa (32 nM)		25-kDa HA (32 nM)	$(6.3 \pm 0.3) \times 10^6$	$(4.7 \pm 0.5) \times 10^6$	$(2.8 \pm 0.3) \times 10^3$	$(2.4 \pm 0.5) \times 10^3$
plasmin (400 nM)	S2251 (0.1 mM)		$(8.0 \pm 0.1) \times 10^2$	$(7.4 \pm 0.3) \times 10^2$	$(7.6 \pm 0.1) \times 10^2$	$(6.9 \pm 0.2) \times 10^2$
		pent. (400 nM)	$(7.3 \bullet 0.3) \times 10^4$	$(6.7 \pm 0.2) \times 10^4$	$(7.8 \pm 0.2) \times 10^2$	$(6.7 \pm 0.3) \times 10^2$
		25-kDa HA (400 nM)	$(7.5 \pm 0.3) \times 10^4$	$(6.5 \pm 0.5) \times 10^4$	$(8.1 \pm 0.4) \times 10^2$	$(7.3 \pm 0.5) \times 10^2$

[a] The table shows the effect of pentasaccharide (pent.) and 25-kDa low-affinity (25-kDa LA) and 25-kDa high-affinity (25-kDa HA) heparins on the rates of inhibition of thrombin, factor Xa, and plasmin by wild-type ATIII, ATIII Rouen I at pH 6, ATIII Rouen I at pH 8, and ATIII Geneva.

values (Table II). The pentasaccharide sequence was sufficient to give maximal activation of factor Xa and plasmin inhibition by wild-type ATIII, whereas full-length heparin is required to give maximal activation of the ATIII–thrombin interaction. Both ATIII Geneva and ATIII Rouen I at pH 8 lost pentasaccharide activation, while Rouen I at pH 6.0 showed essentially normal activity and responded to pentasaccharide. As a control, the inhibition kinetics of ATIII Toyama (47Arg → Cys) was also determined at both pH 6 and pH 8. At both pH values, the mutant behaved identically to ATIII Rouen I at pH 8 (data not shown), in that there was not pentasaccharide activation.

The effect of heparin on the inhibition of the three proteases by ATIII was further characterized by analyzing the initial rate of reaction in the presence of increasing concentrations of several heparin species (Figure 2). Thrombin inhibition by the 6-, 18-, and 25-kDa heparin species occurs as a bell-shaped curve, with optimal inactivation at 1:1 ratios of heparin:ATIII. The pentasaccharide had a further small effect, with the curve being sigmoidal with a midpoint at 1:1 heparin:ATIII concentrations. There was no decrease in the maximum rate of ATIII–thrombin interaction even at very high concentrations of pentasaccharide (Figure 2a).

The inhibition curves for the ATIII–factor Xa interaction (Figure 2b) with both pentasaccharide and high-affinity heparin were also sigmoidal, with the HA species producing a slightly increased rate of inhibition at high concentrations. Profiles for the ATIII–plasmin reaction were similar, except that the curves obtained with both pentasaccharide and high-affinity heparin species were identical.

The pentasaccharide therefore has a small effect on the rate of thrombin inhibition by ATIII. The mechanism of this interaction was further analyzed by utilizing other heparinoid species in conjunction with the pentasaccharide (Table III). This demonstrated that addition of pentasaccharide and low-affinity heparin together gave a k_{ass} of 2.7×10^6 M^{-1} s^{-1}, far higher than the effect of either individually, and only 30-fold less than the effect of 25-kDa high-affinity heparin. Addition of highly sulfated dermatan sulfate disaccharides in conjunction with pentasaccharide was also found to enhance the rate of association between ATIII and thrombin, with a maximum k_{ass} of 5.5×10^5 M^{-1} s^{-1} at a ratio of 4 disaccharide molecules per molecule of ATIII, this being virtually identical to the effect of 14-mer (5-kDa) high-affinity heparin ($k_{ass} = 7.6 \times 10^5$ M^{-1} s^{-1}). This effect was also duplicated by the addition of pentasaccharide in the presence of 0.5 M Cl^- ions ($k_{ass} = 1.4 \times 10^5$ M^{-1} s^{-1}).

Other investigators have demonstrated (Nordenman & Björk, 1978; Oosta et al., 1981) that ATIII undergoes a conformational change on binding to heparin. These studies were extended here to observe the effects of the various heparin species on ATIII conformation, as measured by CD (Figure 3). Heparin induces no changes in the ATIII profile in the far-UV region (190–260 nm, data not shown), but dramatic changes were observed in the near-UV region (260–320 nm), produced by major perturbations in the environments of tryptophan and tyrosine residues. Binding of high-affinity heparin produced an increase in ellipticity, but this was significantly less than the increase produced by the pentasaccharide sequence. Low-affinity heparin in contrast produced only a small increase in overall ellipticity.

Heparin not only produces a conformational change in ATIII but also increases its thermal stability (Fish et al., 1985; Busby et al., 1981). This phenomenon was further examined by comparing the effects of pentasaccharide, 25-kDa high-affinity heparin, and dextran sulfate on the stability of ATIII at 60 °C (Figure 4). The 25-kDa high-affinity heparin produced a large increase in the thermal stability of

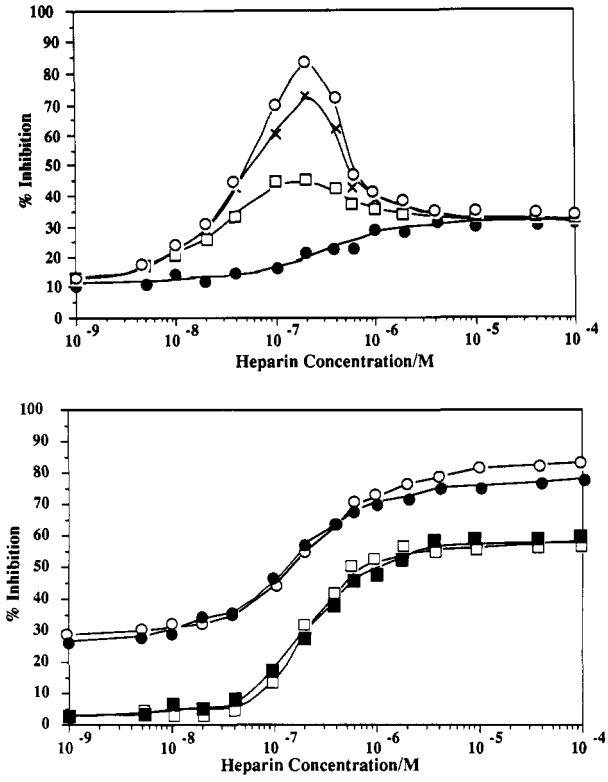

FIGURE 2: Effect of heparin on inhibition by ATIII. Curves show the effect of increasing heparin concentrations on the inhibition of (a, top) thrombin, using (○) 25-kDa high-affinity heparin, (×) 18-kDa high-affinity heparin, (□) 6-kDa high-affinity heparin, and (●) pentasaccharide. (b, bottom) Factor Xa with (○) 25-kDa high-affinity heparin and (●) pentasaccharide and plasmin with (□) 25-kDa high-affinity heparin and (■) pentasaccharide.

Table III: Effects of Heparin Fragments and Cl^- on Thrombin Inhibition[a]

thrombin concentration (nM)	glycosaminoglycan or Cl^- (final molarity)	k_{ass} (M^{-1} s^{-1}) (mean ± SE)
53		(5.5 ± 0.3) × 10^3
53	ΔUA (53 nM)	(1.7 ± 0.4) × 10^4
53	ΔUA (200 nM)	(2.0 ± 0.2) × 10^4
53	25-kDa LA (53 nM)	(2.2 ± 0.2) × 10^4
53	pent. (53 nM)	(6.4 ± 0.2) × 10^4
20	pent. (20 mM)+ΔUA (20 nM)	(6.1 ± 0.4) × 10^4
20	pent. (20 mM)+ΔUA (40 nM)	(2.5 ± 0.3) × 10^5
20	pent. (20 mM)+ΔUA (60 nM)	(3.5 ± 0.5) × 10^5
20	pent. (20 mM)+ΔUA (80 nM)	(5.5 ± 0.3) × 10^5
20	pent. (20 mM)+ΔUA (10 nM)	(5.0 ± 0.4) × 10^5
20	14-mer HA (20 nM)	(7.6 ± 0.2) × 10^5
20	pent. (20 mM) + LA (20 nM)	(2.7 ± 0.5) × 10^6
20	25-kDa HA (20 nM)	(8.7 ± 0.5) × 10^7
42	0 M Cl^-	(4.7 ± 0.3) × 10^3
42	0.2 M Cl^-	(4.9 ± 0.2) × 10^3
42	2.0 M Cl^-	(1.1 ± 0.4) × 10^4
42	0 M Cl^- + 42 nM pent.	(1.4 ± 0.3) × 10^4
42	0.2 M Cl^- + 42 nM pent.	(6.6 ± 0.5) × 10^4
42	0.5 M Cl^- + 42 nM pent.	(1.4 ± 0.2) × 10^5

[a] The table compares the effects of several heparin species, dermatan sulfate derived disaccharide ΔUA→GalNac-4s,6s (ΔUA), 25-kDa low-affinity heparin (LA), pentasaccharide (pent.), 14-mer high-affinity heparin (14-mer HA), 25-kDa high-affinity (HA) heparin, and Cl^- ions on the rate of inhibition of thrombin by ATIII.

ATIII, so that the protein became stable for 8 h at 60 °C. This effect was also seen with pentasaccharide, but not with dextran sulfate or low-affinity heparin. Heparin induced only minimal stabilization of α_1-antitrypsin.

Effect of Heparin on ATIII Cleavage. Jordan et al. (1987) demonstrated that heparin greatly enhanced the rate of ATIII cleavage by human neutrophil elastase. In this study, the effect of heparin and/or pentasaccharide on the rate of ATIII cleavage by human neutrophil elastase, *P. aeruginosa* elastase, and porcine pancreatic elastase were determined. Samples were analyzed both on SDS–PAGE and by loss of inhibitory capacity. Cleavage positions in both the presence and absence of heparin were determined as described in Materials and Methods. N-Terminal sequence analysis of human neutrophil elastase cleaved antithrombin yielded two sequences of equivalent yield (43 pmol), one corresponding to the native N-terminus and the second corresponding to cleavage at the peptide bond Ile380–Ala381. *P. aeruginosa* elastase also yielded two sequences (31 pmol each), corresponding to the native N-terminus of the molecule and to cleavage at the peptide bond Ser384–Leu385. Analysis of porcine pancreatic elastase cleaved antithrombin also yielded two sequences of equivalent yield (28 pmol), corresponding again to the native N-terminus and to cleavage at the peptide bond Val379–Ile380. No other cleavages were detected. Values of K_M, V_{max}, and k_2 for the reactions were determined and are shown in Table IV. This demonstrated that, in each case, heparin had a rate-enhancing effect on the cleavage reaction; the enhancement with porcine pancreatic elastase was small but repeatedly reproducible.

Effect of ATIII Conformation on Heparin Affinity. Recent identification of the latent (L) form of antithrombin (Carrell et al., 1991) and the use of synthetic peptides to produce ATIII binary complexes have provided novel conformations for study. The heparin affinities of these forms for both high-affinity and heterogeneous heparin–Sepharose were determined (Figure 5).

Both L and BC forms of ATIII behaved in a manner similar to that of the cleaved form, in that they had lost high affinity for heterogeneous heparin–Sepharose and all affinity for high-affinity heparin–Separose.

Analyses of the affinity of the mutants Rouen I (47Arg → His) and Geneva (129Arg → Gln) for heparin–Sepharose also provided interesting results (Figure 5). At pH 8, Rouen I had low affinity for heparin–Sepharose, eluting at 0.3 M NaCl, slightly higher than cleaved ATIII, whereas at pH 6, heparin affinity returned to normal (in contrast, ATIII Toyama (Arg47 → Cys) had low affinity at both pH 8 and pH 6 [data not shown]). ATIII Geneva had very low heparin affinity and eluted from the column at 0.05 M NaCl. Thus, it had an affinity even lower than that of cleaved wild-type ATIII.

Effect of Heparin on Binary Complex and Polymer Formation. Binary complexes are formed (Schulze et al., 1990) by the insertion of a synthesized peptide corresponding to the reactive center sequence of ATIII into its A-β-sheet between strands s3A and s5A. The effect of heparin and the pentasaccharide on this process was determined by following the rate of ATIII inactivation and by electrophoresis on nondissociating PAGE (Figure 6).

Both pentasaccharide and high-affinity heparin reduced the rate of peptide insertion into ATIII but had no effect on the rate of insertion into α_1-AT (Table V). The effect of increasing concentrations of pentasaccharide on the rate of peptide A insertion into ATIII shows a sigmoidal relationship (Figure 7), with maximal effect at a ratio of 1.2 mol of pentasaccharide/mol of ATIII.

A special case of binary complex formation is serpin polymerization, were concatomers are formed by the insertion of the reactive center of one molecule into the A-sheet of another (Evans, 1991). The rate of ATIII polymerization was compared in both the presence and absence of pentasac-

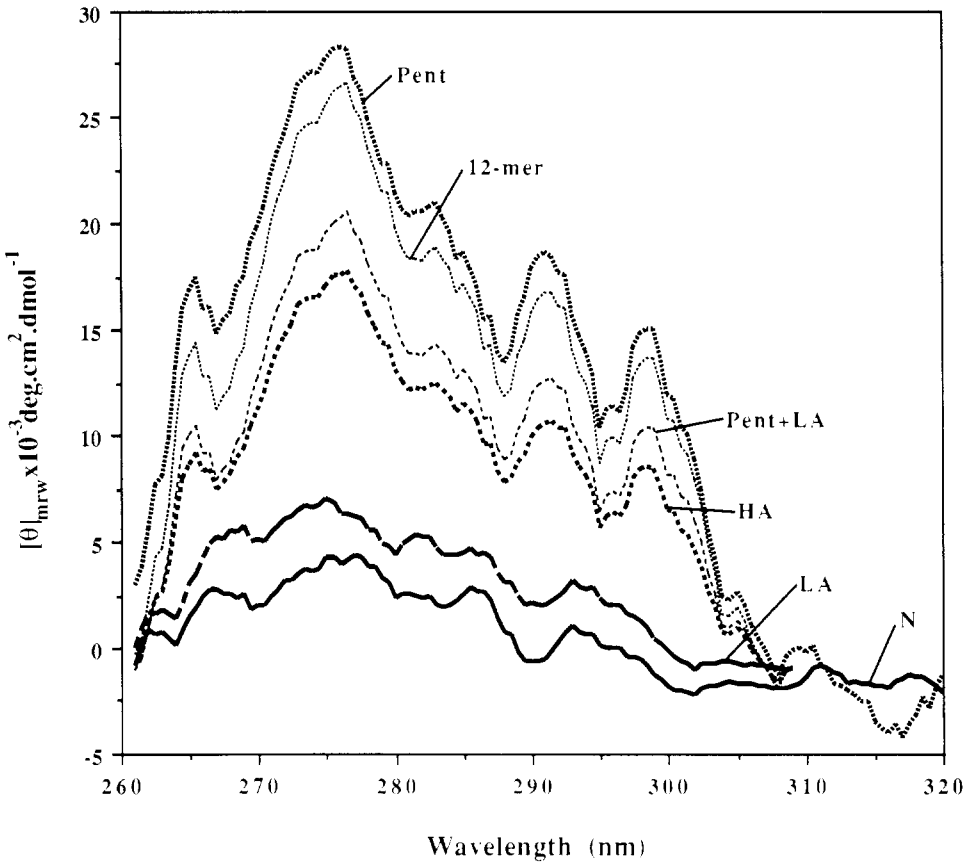

FIGURE 3: CD profiles for heparinized ATIII: near-UV CD analyses of antithrombin with a range of heparin species. Abbreviations: N, native, un-heparinized ATIII; LA, ATIII + 25-kDa low-affinity heparin; HA, ATIII with 25-kDa high-affinity heparin; 12-mer, ATIII + 12-saccharide-unit high-affinity heparin; Pent, ATIII + pentasaccharide.

charide (Figure 8). Again, pentasaccharide had a significant effect in reducing the rate of polymerization of ATIII but had no effect on α_1-antitrypsin polymerization.

DISCUSSION

The sequence alignments shown in Figure 1 support the earlier proposal of a common binding site in the heparin-activated serpins and confirm that the site is present in PAI-1 as well as ATIII, HCII, and PNI. It is formed by the positive face of the D-helix and has dimensions that match those of the smallest high-affinity fraction of heparin—the pentasaccharide. Protein C inhibitor, although a heparin-activatable serpin, does not share the D-helix binding motif (Figure 1) and has recently been shown to bind heparin on the H and A+ helices (Kuhn et al., 1990). A less strongly conserved but consistent feature of the heparin activated serpins is an extension of the positive charge from the D-helix toward the reactive center pole of the molecule (Table I). When projected onto a model of antithrombin (Figure 9), this gives a heparin binding site extending from the N-terminus, along the D-helix up to the proposed position of the reactive center in the inhibitory form. This is compatible with the previous identification of the involvement of residue 114 in antithrombin (Liu & Chang, 1987) and residue 173 in heparin cofactor II (Whinna et al., 1991), of the region 104–251 of antithrombin (Rosenfeld & Danishefsky, 1986), and of residues Lys136 (Chang, 1989), Lys257, and Lys275 (Peterson, et al., 1987) as being involved in heparin binding.

Although the four serpins share a common binding site for heparin, they differ considerably in their mechanism of activation (Evans et al., 1991). Here we examine in detail the activation of antithrombin and its interaction with heparin. The evidence supports a 3-fold mechanism: a conformational activation induced by the pentasaccharide component of high-affinity heparin, ternary complex formation induced by high molecular weight heparin, and a charge neutralization on antithrombin inducible by low-affinity heparin fragments.

Analyses of the effect of increasing concentrations of heparin of various sizes on the initial rate of thrombin inhibition (Figure 2) gave bell-shaped curves typical of the ternary complex model of interaction (Danielsson et al., 1986; Griffith, 1982; Pomerantz & Owen, 1978), where heparin acts as a template to which both ATIII and thrombin bind. The ascending limb represents the formation of increasing amounts of ATIII–heparin complex, to which thrombin can bind and diffuse along, forming a final ternary ATIII–heparin–thrombin complex. The apex represents the maximal rate of inhibition, occurring at a 1:1 ratio of heparin:ATIII. At high concentrations of heparin, the binding sites on both ATIII and thrombin become saturated. They are therefore sterically blocked from interacting with one another, so that the rate of inhibition should fall to the level in the absence of heparin.

This complete decline in the presence of excess heparin was not observed, however, since the initial rate fell to a final level which was still higher than the initial level in the absence of heparin. If the pentasaccharide was used instead of full-length heparin, there was a sigmoidal increase in the rate of inhibition, which reached a plateau at high concentrations. This matched the difference between ATIII in the absence of heparin and ATIII in the presence of high concentrations of high-affinity heparin. Bell-shaped curves due to the ternary complex mechanism are therefore overlaid on the sigmoidal curve due to the pentasaccharide, showing that two processes are involved: basal conformational activation as with the

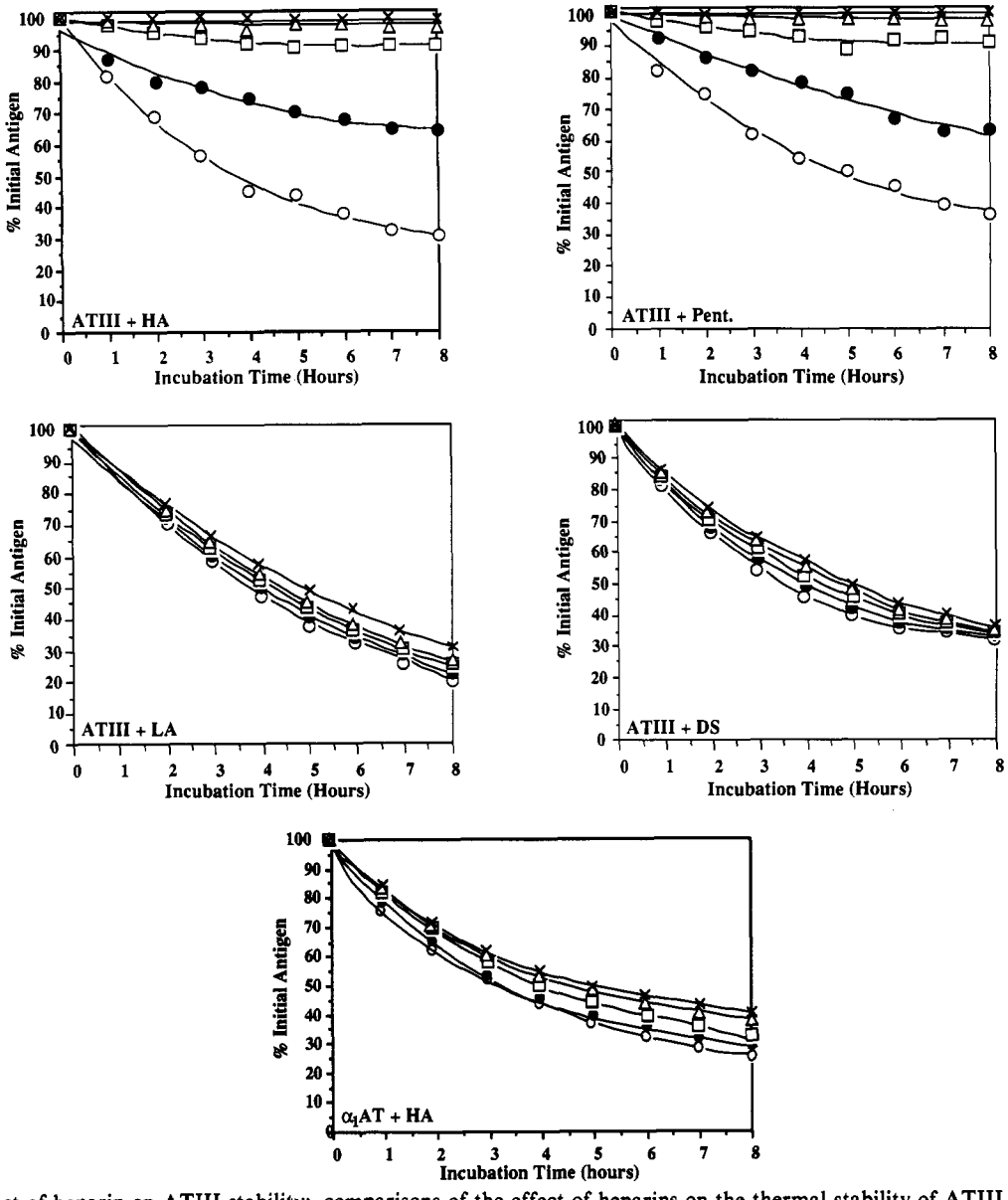

FIGURE 4: Effect of heparin on ATIII stability: comparisons of the effect of heparins on the thermal stability of ATIII at 60 °C. (a, top left) ATIII + 25-kDa high-affinity heparin; (b, top right) ATIII + pentasaccharide; (c, middle left) ATIII + 25-kDa low-affinity heparin; (d, middle right) ATIII + 15-kDa dextran sulfate; (e, bottom) α_1-AT + 25-kDa high-affinity heparin. In each case the following molar ratios of glycosaminoglycan:ATIII were used: 0:1 (○), 0.05:1 (●), 0.5:1 (□), 1:1 (△), and 10:1 (×); the resultant solutions were incubated at 60 °C for up to 8 h, with remaining soluble protein determined by rocket immunoelectrophoresis.

Table IV: Effect of Heparin on ATIII Cleavage[a]

protease	heparin species	K_M (M)	V_{max} (M s^{-1})	k_2 (s^{-1})
HNE				
HNE	25-kDa HA	5.7×10^{-6}	6.4×10^{-8}	2.4
HNE	pentasaccharide	2.7×10^{-3}	5.4×10^{-10}	0.02
PsE		15×10^{-6}	5.3×10^{-9}	1.9
PsE	25-kDa HA	4×10^{-6}	1.8×10^{-8}	6.4
PsE	pentasaccharide	4.8×10^{-6}	1.4×10^{-8}	5.1
PPE		2.7×10^{-6}	1.9×10^{-9}	0.03
PPE	25-kDa HA	1.9×10^{-6}	4.3×10^{-9}	0.05
PPE	pentasaccharide	1.8×10^{-6}	3.8×10^{-9}	0.05

[a] Comparison of high-affinity (HA) heparin and pentasaccharide on the rate of antithrombin cleavage by human neutrophil elastase (HNE), *Pseudomonas aeruginosa* elastase (PsE), and porcine pancreatic elastase (PPE).

pentasaccharide and a predominant ternary effect involving linkage of the thrombin to the antithrombin.

A prediction from the ternary complex mechanism of interaction is that the longer the heparin fragment, the greater the rate enhancement, as it will predictably form a more efficient bridge. This was indeed observed, with 25-kDa high-affinity heparin having the greatest enhancement effect and 6-kDa high-affinity heparin having the smallest effect. Both pentasaccharide and full-length heparin produced a sigmoidal increase in the rate of inhibition of factor Xa by ATIII, though the maximum rate produced by full-length heparin was higher, due to a small contribution of the ternary complex mechanism, as factor Xa binds heparin with low affinity. A similar sigmoidal increase in the rate of inhibition with increasing concentrations of both pentasaccharide and high-affinity heparin was observed for the inhibition of plasmin by ATIII. There was no ternary complex effect in this case as plasmin does not bind heparin. The effect of heparin on the inhibition of both factor Xa and plasmin is therefore similar to the effect of pentasaccharide on thrombin inhibition. However, the additional activation that occurs with thrombin with high affinity (high molecular weight) heparin, i.e., the ternary complex diffusion effect, is minimal with factor Xa as

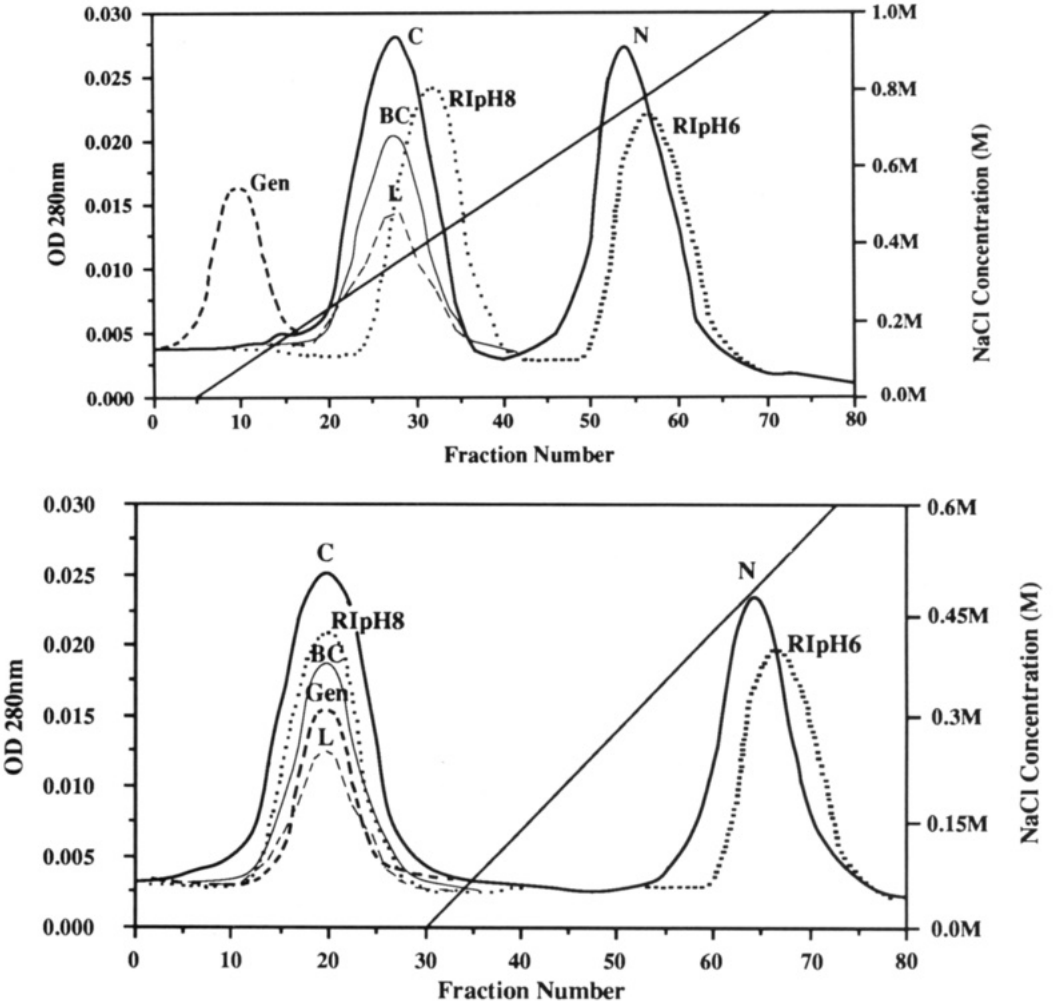

FIGURE 5: Heparin–Sepharose elution profiles for ATIII species. Elution profiles are shown from (a, top) heterogeneous heparin–Sepharose and (b, bottom) high-affinity heparin–Sepharose of binary complexed antithrombin (BC and thin line), latent L antithrombin (L and thin dashed line), and the mutants Geneva (Arg128 → Gln) (Gen and dashed line), Rouen I (47Arg → His) at pH 6.0 (RIpH6 and large dots) and Rouen I at pH 8.0 (RIpH8 and small dots) in comparison to native (N) and reactive center cleaved (C) wild-type antithrombin.

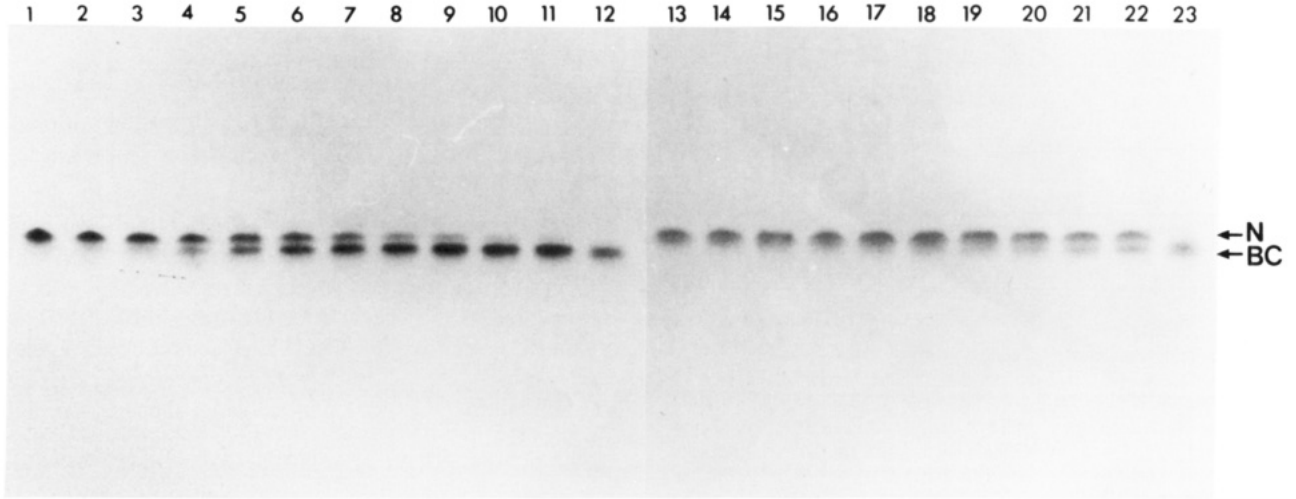

FIGURE 6: Peptide insertion into ATIII. The nondissociating PAGE gel shows the effect of heparin on the rate of peptide C insertion into ATIII. Lanes 1 and 13: native wild-type ATIII. Lanes 2–12: aliquots removed at 5, 10, 15, 30, 45, 60, 75, 90, 120, 240, 360, and 720 min after incubation at 37 °C of 100:1 molar ratio of peptide C with ATIII. Lanes 14–23 are identical to lanes 2–11 excpet that incubation was with pentasaccharide at a 1:1 molar ratio with ATIII (N, native ATIII; BC, binary complex).

characterized by the weak dissociation constant of 140 μM (Craig et al., 1989) and is not seen with plasmin.

The effects of various heparin species on antithrombin were further examined by circular dichroism studies (Figure 3). As described by Stone et al. (1982), heparin species of 12 saccharide units and 25-kDa high-affinity heparin gave different spectra, with the spectrum due to 25-kDa high-affinity heparin having reduced ellipticity compared to the spectrum with the 12-mer. By comparison, the pentasaccharide gave essentially the same transition as the 12-mer,

Table V: Effect of Heparin on Peptide Insertion into ATIII[a]

serpin	peptide	heparin species	k_{obs} (M^{-1} s^{-1})
ATIII	A		9.7×10^{-2}
ATIII	A	25-kDa LA	6.1×10^{-2}
ATIII	A	25-kDa HA	8.2×10^{-3}
ATIII	A	pentasaccharide	4.3×10^{-3}
ATIII	C		13.1×10^{-2}
ATIII	C	25-kDa LA	12.4×10^{-2}
ATIII	C	25-kDa HA	4.4×10^{-2}
ATIII	C	pentasaccharide	3.7×10^{-2}
α_1-AT	C		15.4×10^{-2}
α_1-AT	C	25-kDa HA	13.8×10^{-2}
α_1-AT	C	pentasaccharide	14.3×10^{-2}

[a] Comparison of the effects of 25-kDa low-affinity (LA) and 25-kDa high-affinity (HA) heparins and pentasaccharide on the rate of peptide A and C insertion into ATIII and α_1-antitrypsin.

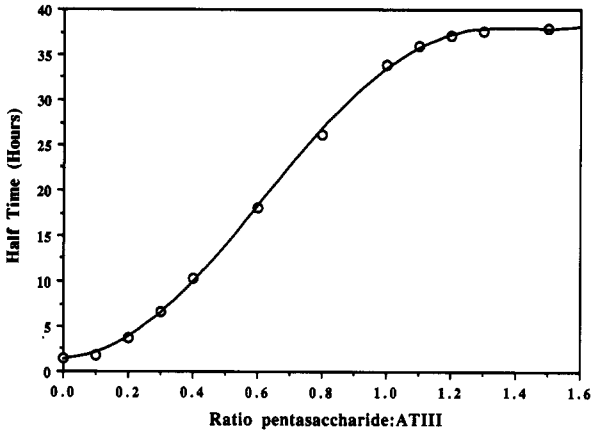

FIGURE 7: Heparin dependence of peptide insertion into ATIII. The curve shows the effect of increasing pentasaccharide concentrations on the half-time of peptide A insertion into ATIII, as measured by the loss of ATIII inhibitory activity at each concentration of pentasaccharide.

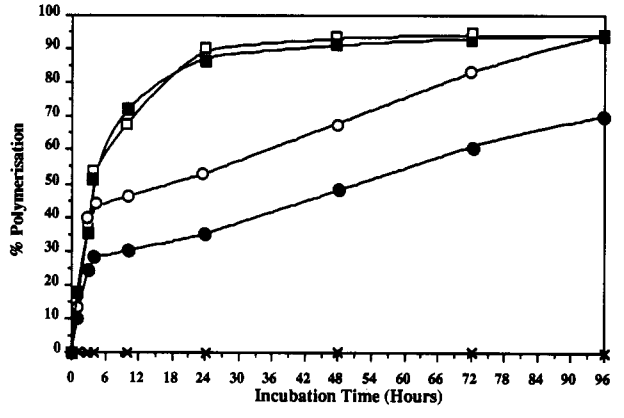

FIGURE 8: Heparin dependence of ATIII polymerization: comparison of the effect of pentasaccharide on the rate of ATIII and α_1-antitrypsin polymerization at 65 °C. The curves shown are (□) native α_1-antitrypsin, (■) α_1-antitrypsin with equimolar pentasaccharide, and (○) native ATIII and (●) ATIII with equimolar pentasaccharide. Also shown for comparison is ATIII binary complex (×), which does not polymerize. The degree of polymerization at each time point was determined by size-exclusion chromatography on a TSK2000 gel.

whereas low-affinity heparin induced only a minor increase in ellipticity, indicating that pentasaccharide binding is responsible for the major component of the heparin-induced conformational change. When a mixture of low-affinity heparin and pentasaccharide was used, the resultant CD profile was essentially the same as that produced by 25-kDa high-affinity heparin, indicating that the binding of two separate components of the heparin molecule is responsible for the profile of 25-kDa high-affinity heparin and that both pentasaccharide and a low-affinity species contribute to the overall ellipticity.

Thus, pentasaccharide binding induces a conformational change in ATIII and is associated with a dramatic 300-fold increase in the affinity of ATIII for heparin (Olsen et al., 1981). Analyses of ATIII mutants with reduced heparin affinities have provided the opportunity to identify those residues in ATIII responsible for binding to the pentasaccharide.

Identification of the Pentasaccharide Binding Site. Several low-heparin-affinity mutants of ATIII involve changes to the residue Arg47 (Owen et al., 1987; Borg et al., 1988; Koide et al., 1984). An interesting variant is ATIII Rouen I (Arg47 → His), as the charge carried by the histidine can be varied by altering the pH.

Affinity of the mutant was determined for heparin–Sepharose (Figure 5) prepared using either heterogeneous heparin (unfractionated) or a high-affinity fraction (heparin of very low molecular weight fractionated on the basis of high ATIII affinity so that it corresponds to little more than the pentasaccharide). At pH 6.0, with the histidine protonated, ATIII Rouen I bound to both heterogeneous and high-affinity heparin–Sepharose with normal affinities, equivalent to 0.8 and 0.55 M NaCl, respectively. In contrast, at pH 8.0 with the histidine residue deprotonated, affinity for heterogeneous heparin–Sepharose fell to 0.4 M NaCl, while affinity for high-affinity heparin–Sepharose was completely lost.

Kinetic analyses (Table II) also demonstrated that at pH 6.0 ATIII Rouen I behaved as wild-type ATIII. In both cases, low-affinity heparin increased the rate of interaction of ATIII and thrombin by a factor of 4. The pentasaccharide had a greater effect on this interaction, producing a 12-fold enhancement, while 25-kDa high-affinity heparin produced maximal enhancement of 16 000-fold.

Pentasaccharide gave a 200-fold enhancement of the ATIII–factor Xa interaction, with 25-kDa high-affinity heparin giving a rate enhancement of 4000-fold, an additional 20-fold effect in addition to that obtained with pentasaccharide. The pentasaccharide and 25-kDa high-affinity heparin each gave a 100-fold enhancement of the ATIII–plasmin interaction.

At pH 8.0, ATIII Rouen I showed no pentasaccharide activation against thrombin, factor Xa, or plasmin. Low-affinity heparin again produced a 4-fold increase in the k_{ass} of the ATIII–thrombin interaction. In this case, however, the 25-kDa high-affinity heparin produced only a 4-fold activation. Thus, when histidine 47 is deprotonated, ATIII Rouen I has lost all affinity for and activation by the pentasaccharide, though the interaction with the low-affinity fraction of heparin is unaffected.

ATIII Basel (Arg129 → Gln) has also lost all affinity for high-affinity heparin–Sepharose, and affinity for heterogeneous heparin–Sepharose is also dramatically reduced, and it elutes at 0.05 M NaCl, a lower concentration than that of cleaved ATIII (Figure 5). Kinetic analyses (Table II) demonstrated that as with ATIII Rouen I at pH 8.0 all pentasaccharide activation was lost and 25-kDa high- and low-affinity heparins only gave a 3-fold activation of the ATIII–thrombin interaction. This indicates that Arg129 is involved in both the pentasaccharide and the low-affinity binding sites, while Arg47 is involved solely in pentasaccharide binding. These findings are in good agreement with the modeling studies of Grootenhuis and van Boeckel (1991).

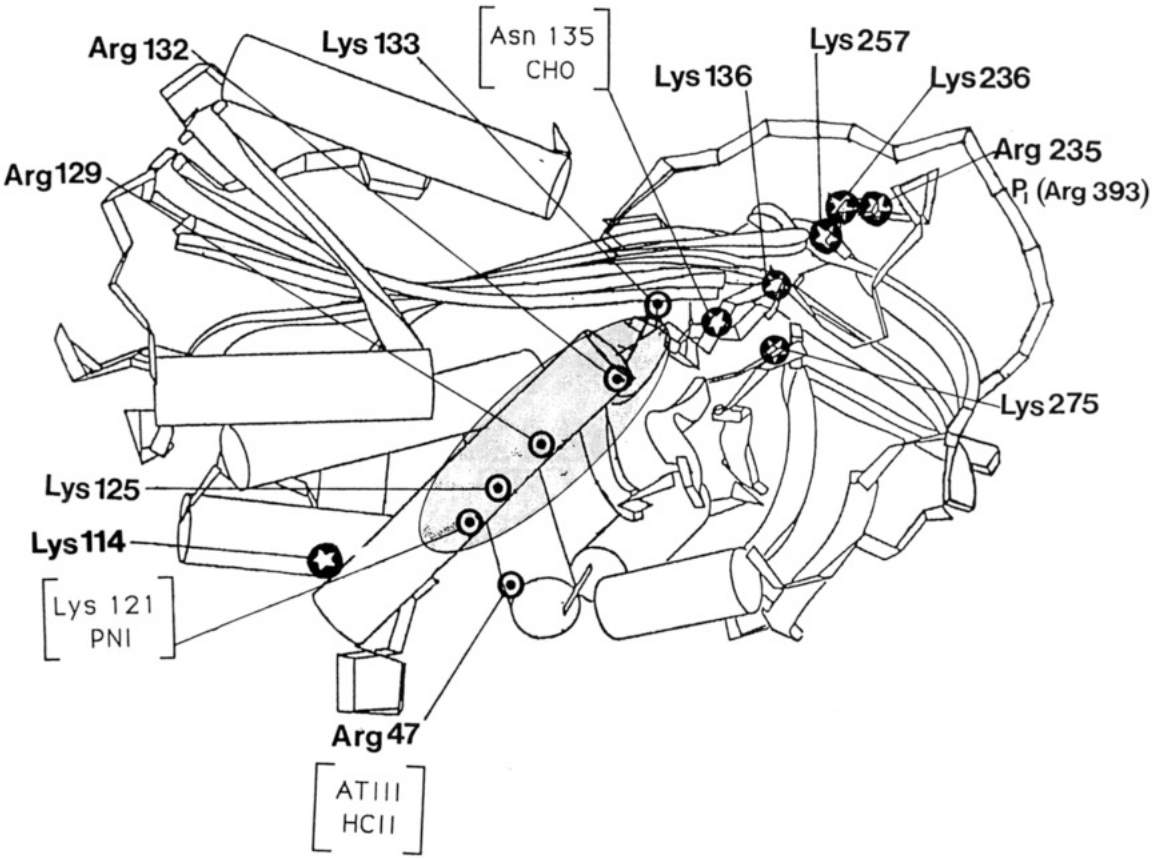

FIGURE 9: Heparin binding site of ATIII. The proposed heparin binding site is shown on a model of native antithrombin on the basis of the α_1-AT and ovalbumin coordinates. Positively charged residues uniquely conserved in ATIII, HCII, PNI, and PAI-1 were found on the D-helix and form the primary site. Arg47 on the A-helix is conserved in ATIII and HCII, while the corresponding residue Lys121 is found in PNI. The model also shows an extended site of positive charge leading from the D-helix to near the reactive center pole of the molecule. The shaded region encompasses the primary pentasaccharide binding site and is equivalent in size to the dimensions of the pentasaccharide (22 Å). The extended site toward the reactive center (P_1 Arg393) is also shown. This is equivalent in size to four disaccharide units (43 Å). On the model, the N-terminal extension is absent.

Consequences of Pentasaccharide Binding. In addition to inducing a conformational change, heparin also enhances the thermal stability of ATIII. Comparisons were made of the effect of high- and low-affinity heparins, pentasaccharide, and dextran sulfate on the stability of ATIII at 60 °C (Figure 4). Both high-affinity heparin and pentasaccharide at 1:1 ratios stabilized ATIII for up to 8 h at 60 °C, whereas low-affinity heparin and dextran sulfate had only minor effects. Heparin also had only a minor stabilizing effect on α_1-AT, demonstrating that the effect of heparin is specific and dependent on the pentasaccharide.

The effects of pentasaccharide on the rate of cleavage of antithrombin by human neutrophil elastase, *P. aeruginosa* elastase, and porcine pancreatic elastase were studied. These proteases were chosen as their affinities for heparin correspond to the heparin affinities of thrombin, factor Xa, and plasma, respectively, in that human neutrophil elastase has high heparin affinity, *P. aeruginosa* elastase has low heparin affinity, and porcine pancreatic elastase does not bind heparin (Christey, 1990).

The rate of ATIII cleavage by human neutrophil elastase was slightly increased in the presence of pentasaccharide and greatly increased in the presence of 25-kDa high-affinity heparin (Table IV), which agrees with the results of Jordan et al. (1989). This corresponds to the effect of pentasaccharide and 25-kDa high-affinity heparin on thrombin inhibition by ATIII (Table II). *P. aeruginosa* elastase cleavage was enhanced 2.7-fold by pentasaccharide (from $k_2 = 1.9\ s^{-1}$ to $5.1\ s^{-1}$) and slightly more by 25-kDa high affinity heparin, to $6.4\ s^{-1}$, which corresponds to the effect of pentasaccharide and high-affinity heparin on the factor Xa–ATIII interaction. Porcine pancreatic elastase cleavage of ATIII was enhanced 1.6 times in the presence of both pentasaccharide and high-affinity heparin (from $k_2 = 0.03\ s^{-1}$ to $0.05\ s^{-1}$), demonstrating the same behavior as seen for the inhibition of plasmin by ATIII.

For both inhibition and cleavage, therefore, the effects of pentasaccharide and high-affinity heparin depend on the relative affinity of the protease for heparin. Thrombin (which has recently been shown by Olsen et al. (1991) to bind strongly, but nonspecifically, to heparin) and human neutrophil elastase with high heparin affinities show little activation by the pentasaccharide and a large degree of activation by high-affinity heparin. Plasmin and porcine pancreatic elastase with no affinity for heparin show the same degree of activation by both pentasaccharide and high-affinity heparin. Factor Xa and *P. aeruginosa* elastase with low heparin affinity show a large degree of activation by pentasaccharide and slightly greater activation by high-affinity heparin. The effect of the pentasaccharide in increasing the rate of cleavage implies that the conformational change associated with its binding is altering the conformation of the reactive center, making it more accessible for both proteolysis and inhibition. As can be seen (Figure 5), on cleavage at the reactive center, ATIII reverts to a low-affinity form, eluting from heterogeneous heparin–Sepharose at 0.3 M NaCl. However, there is no binding at all to high-affinity heparin–Sepharose. This suggests that the pentasaccharide binding site is perturbed

but that the low-affinity site is unchanged. On cleavage, the reactive center site of serpins inserts as the fourth strand in the main A-β-sheet (Löbermann et al., 1984). Other serpin conformations involving insertions into the A-sheet have been characterized (Carrell et al., 1991). The binary complex form (BC) is produced by interaction of the serpin with peptides corresponding to the reactive center sequence. These insert as strand four in the A-β-sheet and induce a conformational change akin to that seen on cleavage. The latent L form is produced by treatment of ATIII with 0.9 M GdmCl overnight at 4 °C (Carrell et al., 1991). A form which is inactive and resembles latent PAI-1 in properties is induced. Figure 5 demonstrates that these two forms resemble cleaved ATIII with regard to their affinity for heterogeneous and high-affinity heparin–Sepharose. Insertions into the A-sheet therefore cause a conformational change in ATIII which reverts the molecule to a low-affinity form.

To examine further the effect of heparin on the reactive center of ATIII, the serpin was reacted with the peptides A (Ac-Ser-Glu-Ala-Ala-Ala-Ser-Thr-Ala-Val-Val-Ile-Ala-Gly-OH) and C (Ac-Ser-Glu-Ala-Ala-Ala-Ser-Thr-Ala-Val-OH), corresponding to parts of its reactive center sequence. Both pentasaccharide and 25-kDa high-affinity heparin greatly reduced the rate of both peptide A and peptide C insertion into ATIII (Figure 6, Table V), with the effect of the pentasaccharide being as great as the effect of high-affinity heparin in both cases. Low-affinity heparin had no effect on the rate of insertion into ATIII, while neither pentasaccharide nor high-affinity heparin had an effect on the rate of peptide insertion into α_1-AT. Thus, the effect of the pentasaccharide on peptide insertion is specific.

The effect of increasing the concentration of pentasaccharide on the half-time of peptide A insertion into ATIII was also measured (Figure 7). The curve produced is sigmoidal, with the half-time of insertion increasing to a maximum at more than 1.2 mol of pentasaccharide/mol of ATIII. This curve is comparable to that produced by increasing concentrations of pentasaccharide in the inhibition of factor Xa by ATIII (Figure 2b), suggesting that the phenomenon occurring is similar, if not the same. A special case of peptide insertion is found in ATIII polymerization (Evans, 1991), where the reactive center of one serpin molecule inserts into the A-sheet of another. The effect of heparin on α_1-antitrypsin and ATIII polymerization at 65 °C was determined (Figure 8). This demonstrates that the pentasaccharide makes polymerization of ATIII more difficult, in effect doubling the time required for full polymerization, but polymerization of α_1-antitrypsin is unaffected. To prolong the time needed for peptides to insert or ATIII to polymerize, there needs to be some steric hindrance in the area of A-sheet. The pentasaccharide is itself too small to affect this region directly, so its effect must be indirect. One way this could arise is if the pentasaccharide induces the reactive center to partially insert into the A-sheet, giving the optimal canonical conformation and thus blocking peptide insertion.

This evidence, along with the observed increases in the rates of proteolysis and inhibition, shows that the pentasaccharide-induced conformational change makes the reactive center more accessible. Complete insertion of the reactive center into the A-sheet, as seen on cleavage, binary complex, or L-form formation, induces a second conformational change which perturbs the pentasaccharide binding site, so that ATIII reverts to a low-affinity form.

The Extended Site. Circular dichroic analyses demonstrated that the pentasaccharide and low-affinity components of heparin had separate effects and that adding both pentasaccharide and 25-kDa low-affinity heparin together gave the same profile as 25-kDa high-affinity heparin (Figure 3). Comparisons of affinities for high-affinity and heterogeneous heparin–Sepharose show that perturbation of the pentasaccharide site induces complete loss of affinity for high-affinity heparin–Sepharose, whereas some affinity for heterogeneous heparin–Sepharose is retained, again indicating a difference between the pentasaccharide and low-affinity binding sites. These results support the existence of a secondary binding site extending beyond the pentasaccharide site. Kinetic analyses were performed to examine the behavior of the pentasaccharide and low-affinity sites in more detail.

Highly sulfated disaccharides obtained from dermatan sulfate were added in conjunction with pentasaccharide, and their effect on thrombin inhibition was measured (Table III). By themselves, the disaccharides had only a 3-fold effect on the rate of reaction (raising the k_{ass} from 5.5×10^3 to 1.7×10^4 M^{-1} s^{-1}), whereas the pentasaccharide had a 10-fold effect (to 6.4×10^4 M^{-1} s^{-1}). Addition of disaccharide to a ratio of 4:1 together with pentasaccharide gave a maximal k_{ass} of 5.5×10^5 M^{-1} s^{-1}, a 100-fold rate enhancement. This corresponded to the k_{ass} with 14-mer high-affinity heparin (k_{ass} = 7.6×10^5 M^{-1} s^{-1}), and makes antithrombin as good a thrombin inhibitor as the Pittsburg (383Met → Arg) variant of α_1-antitrypsin (George et al., 1989). The effect of low-affinity heparin was also examined. By itself it gave a k_{ass} of 2.2×10^4 M^{-1} s^{-1}, a 4-fold enhancement, but when added in conjunction with pentasaccharide this increased to 2.7×10^6 M^{-1} s^{-1}, a 490-fold enhancement and only 30-fold less than the maximal k_{ass} produced by high-affinity heparin (8.7×10^7 M^{-1} s^{-1}). These findings suggested the presence of a second extended heparin binding site, which must be blocked before thrombin can adequately dock. Strong evidence for this came from studies in the effects of Cl^- ions on activation (Table III). For these studies, $MnCl_2$ was chosen, as Mn^{2+} is a weak cation and is therefore unlikely to participate in the reaction. Low levels of Cl^- (from 0 to 0.2 M) produced no effect on the rate of thrombin inhibition by antithrombin, but at 2 M Cl^- there was a 2-fold increase in k_{ass} from 1.7×10^3 M^{-1} s^{-1} to 1.1×10^4 M^{-1} s^{-1}, only 2-fold less than the effect of low-affinity heparin. A more marked effect was seen with pentasaccharide, with the k_{ass} increasing from 1.4×10^4 M^{-1} s^{-1} at 0 M Cl^- to 6.6×10^4 M^{-1} s^{-1} at 0.2 M Cl^- to 1.4×10^5 M^{-1} s^{-1} at 0.5 M Cl^-. Thus at 0.5 M Cl^-, the inhibition of thrombin in the presence of pentasaccharide is only 3-fold less efficient than inhibition by 14-kDa high-affinity heparin. The pentasaccharide thus induces a conformational change which is necessary for thrombin to dock. This leaves the extended site exposed, the charge on which can be negated by the addition of Cl^- ions, thus allowing charged proteases to approach and dock. The necessity of the initial pentasaccharide-induced conformational change explains why Cl^- ions alone produce little or no activation at low concentrations (Markovich et al., 1979; Petersen & Jørgensen 1983; Olsen & Björk, 1991).

There has recently been considerable discussion by others of the relationship of the reactive center loop of the serpins to the A-sheet and the changes that take place to give the active inhibitory conformation (Engh et al., 1990; Skriver et al., 1991; Mast et al., 1992; Schulze et al., 1992). In particular, evidence has been presented for the conformational change that takes place on addition of heparin to antithrombin (Carrell et al., 1991; Björk et al., 1992). Taken together with the evidence in this paper, it is concluded that heparin has a 3-fold action (Figure 10). ATIII is secreted in a form which is an

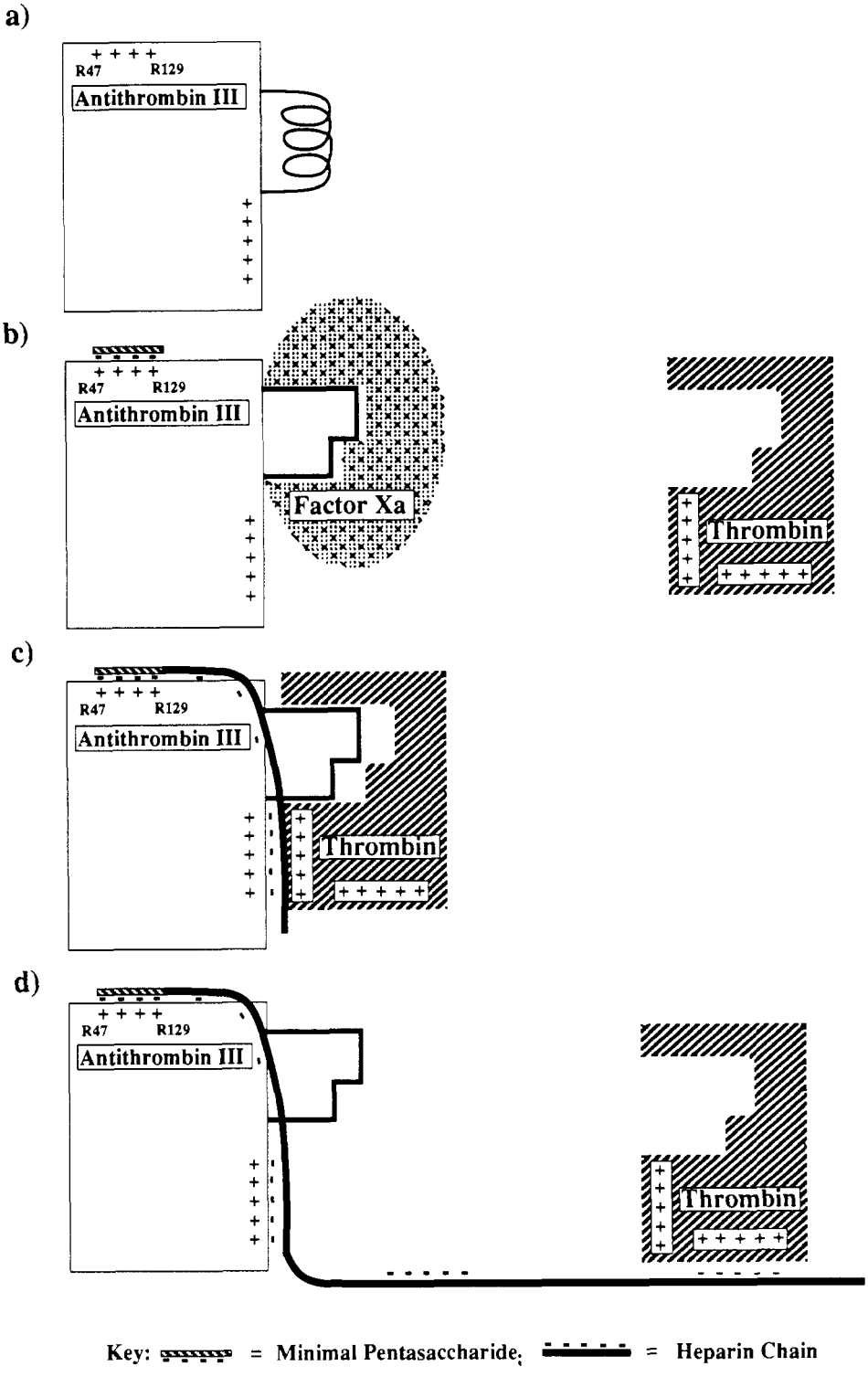

FIGURE 10: Model for heparin activation of ATIII: schematic diagram showing the three mechanisms involved in the heparin activation of ATIII. (a) Native unheparinized ATIII is shown, where the reactive center is in an inaccessible conformation. (b) The pentasaccharide induces a conformational change, making the reactive center more accessible. This leaves the extended site uncovered, so that only uncharged or slightly charged proteases such as plasmin or factor Xa can readily approach. (c) A longer heparin chain (up to 14 residues) can induce the conformational change and cover the extended site, thus allowing charged proteases to approach more readily. (d) Even longer heparin chains—up to a maximum size of 25-kDa—extend from the ATIII molecule, providing a charged conduit to which the thrombin molecule can bind and diffuse along, thus providing the ternary complex/template mechanism of interaction.

ineffective inhibitor and a poor substrate, suggesting that the reactive center is inaccessible. The pentasaccharide induces a conformational change, with an associated increase in heparin affinity and thermal stability. This is compatible with partial reinsertion of the reactive center into the A-sheet of the molecule, with a shift of the reactive center from the inaccessible conformation into an optimal inhibitor "canonical" conformation (Figure 10b). The extended heparin binding site (Figure 9) remains uncovered, so that only uncharged or slightly positively charged proteases (factor Xa, plasmin, porcine pancreatic elastase, *P. aeruginosa* elastase) can readily approach the ATIII molecule to complex with it, or to cleave it. Charged proteases (thrombin, human neutrophil elastase) are repelled by the high positive charge density, so that only

a small increase in the rate of association is produced by the pentasaccharide (10-fold for the ATIII–thrombin interaction). A 14-mer heparin species (corresponding to pentasaccharide with four disaccharides) is sufficiently long to cover the extended binding site, negating the charge repulsion and allowing thrombin to dock (Figure 10c), producing a further 10-fold enhancement of the ATIII–thrombin interaction.

Longer chains of heparin extend off the ATIII molecule (Figure 10d), providing a charged conduit to which thrombin can bind and diffuse along to finally dock with the ATIII. This is the ternary complex mechanism of activation (Danielsson et al., 1986) and works by both increasing the probability of the ATIII and thrombin coming into contact and stabilizing the ATIII–heparin–thrombin ternary complex producing an additional 174-fold effect over and above that seen with pentasaccharide and 14-mer heparin species. This effect can be seen to varying degrees with all proteases which have some affinity for heparin, in that 25-kDa high-affinity heparin enhances the rate of inhibition and cleavage to a greater extent than the pentasaccharide. The largest effect is seen with highly postively charged proteases, such as thrombin and human neutrophil elastase, where binary complex formation plays the predominant part in the inhibitory mechanism.

The evidence therefore supports a common heparin binding site in all four heparin–activatable serpins, with antithrombin activation occurring by a 3-fold mechanism, a pentasaccharide-induced conformational change, charge neutralization of the extended binding site, and ternary complex formation on extended heparin chains.

ACKNOWLEDGMENT

We thank Dr. L. C. Packmann for performing the sequence analyses. We also thank Dr. J. Choay for the gift of the heparin pentasaccharide and Dr. J.-M. Freyssinet for the human thrombin. D.Ll.E. is an Elmore Fellow.

REFERENCES

Beatty, K., Bieth, J., & Travis, J. (1980) *J. Biol. Chem. 255*, 3931–3934.

Björk, I., Ylinenjärvi, K., Olson, S. T., & Bock, P. E. (1992) *J. Biol. Chem. 267*, 1976–1982.

Borg, J.-Y., Owen, M. C., Soria, C., Soria, J., Caen, J., & Carrell, R. W. (1988) *J. Clin. Invest. 81*, 1292–1296.

Brennan, S. O., Borg, J.-Y., George, P. M., Soria, C., Soria, J., Caen, J., & Carrell, R. W. (1988) *FEBS Lett. 237*, 118–122.

Busby, T. F., Atha, D. H., & Ingham, K. (1981) *J. Biol. Chem. 256*, 12140–12147.

Carrell, R. W., Christey, P. B., & Boswell, D. R. (1987) *Thrombosis and Haemostasis XIth International Conference on Thrombosis and Haemostasis 58*(1).

Carrell, R. W., Evans, D. Ll., & Stein, P. E. (1991) *Nature 353*, 576–578.

Chang, J.-Y. (1989) *J. Biol. Chem. 264*, 3111–3115.

Chase, T., Jr., & Shaw, E. (1969) *Biochemistry 8*, 2212–2224.

Choay, J. (1989) *Sem. Throm. Hemostas. 14*, 359–364.

Choay, J., Petitou, M., Lormeau, J. C., Sinaÿ, P., Casu, B., & Gatti, G. (1983) *Biochem. Biophys. Res. Commun. 116*, 492–499.

Christey, P. B. (1990) Ph.D. Thesis, University Library, University of Cambridge.

Craig, P. A., Olson, S. T., & Shore, J. D. (1989) *J. Biol. Chem. 264*, 5452–5461.

Danielsson, A., Raub, E., Lindahl, U., & Björk, I. (1986) *J. Biol. Chem. 261*, 15467–15473.

Ehrlich, H. J., Keijer, J., Preissner, K. T., Gebbink, R. K., & Pannekoek, H. (1991) *Biochemistry 30*, 1021–1028.

Ellis, V., Scully, M. F., & Kakkar, V. V. (1986) *Biochem. J. 238*, 329–333.

Engh, R. A., Wright, H. T., & Huber, R. (1990) *Protein Eng. 3*, 469–477.

Evans, D. Ll. (1991) Ph.D. Thesis, University Library, University of Cambridge.

Evans, D. Ll., Christey, P. B., & Carrell, R. W. (1990) *Serine Proteases and their Serpin Inhibitors in the Nervous System: Regulation in Development and in Degenerative and Malignant Disease* (Festoff, B. W., Ed.) pp 69–77, Plenum Publishing, London.

Evans, D. Ll., McGrogan, M., Scott, R. W., & Carrell, R. W. (1991) *J. Biol. Chem. 266*, 2307–2312.

Fish, W. W., Danielsson, A., Nordling, K., Miller, S. H., Lam, C. F., & Björk, I. (1985) *Biochemistry 24*, 1510–1517.

Gandrille, S., Aiach, M., Lane, D. A., Vidaud, D., Molho-Sabatier, P., Caso, R., de Moerloose, P., Fiessinger, J.-N., & Clauser, E. (1990) *J. Biol. Chem. 265*, 18997–19001.

George, P. M., Pemberton, P., Bathurst, I. C., Carrell, R. W., Gibson, H. L., Rosenberg, S., Hallwell, R. A., & Barr, P. J. (1989) *Blood 73*, 490–496.

Goldenberg, D. P. (1989) *Protein Structure: A practical approach* (Creighton, T. E., Ed.) pp 225–250, IRL Press, Oxford.

Griffth, M. J. (1982) *J. Biol. Chem. 257*, 7360–7365.

Grootenhuis, P. D. J., & van Boeckel, C. A. A. (1991) *J. Am. Chem. Soc. 113*, 2743–2747.

Holmer, E., Kurachi, K., & Söderström, G. (1981) *Biochem. J. 193*, 395–400.

Höök, M., Björk, I., Hopwood, J., & Lindahl, U. (1976) *FEBS Lett. 66*, 90–93.

Huber, R., & Carrell, R. W. (1989) *Biochemistry 28*, 8951–8966.

Jordan, R. E., Kilpatrick, J., & Nelson, R. M. (1987) *Science 237*, 777–779.

Jordan, R. E., Nelson, R. M., Kilpatrick, J., Newgren, J. O., Esmon, P. C., & Fournel, M. A. (1989) *J. Biol. Chem. 264*, 10493–10500.

Koide, T., Odani, S., Takahashi, K., Ono, T., & Sakuragawa, N. (1984) *Proc. Natl. Acad. Sci. U.S.A. 81*, 289–293.

Kuhn, L. A., Griffin, J. H., Fisher, C. L., Greengard, J. S., Bouma, B. N., España, F., & Tainer, J. A. (1990) *Proc. Natl. Acad. Sci. U.S.A. 87*, 8506–8510.

Lam, L. H., Silbert, J. E., & Rosenberg, R. D. (1976) *Biochem. Biophys. Res. Commun. 69*, 570–576.

Laurell, C. B. (1966) *Anal. Biochem. 15*, 45–52.

Lesk, A. M., Levitt, M., & Chothia, C. (1984) *Protein Eng. 1*, 11–14.

Liu, C.-S. & Chang, J.-Y. (1987) *J. Biol. Chem. 262*, 17356–17361.

Löbermann, H., Deisenhofer, J., Tokuoka, R., & Huber, R. (1984) *J. Mol. Biol. 77*, 531–556.

Lomas, D. A., Evans, D. Ll., Finch, J. T., & Carrell, R. W. (1992) *Nature 357*. 605–607.

Markovich, R., Regoeczi, E., & Hatton, M. W. C. (1979) *Thromb. Res. 15*, 821–834.

Mast, E. A., Enghild, J. J., & Salvesen, G. (1992) *Biochemistry 31*, 2720–2728.

Matsudaira, P. (1987) *J. Biol. Chem. 262*, 10035–10038.

McKay, E. J. (1981) *Thromb. Res. 21*, 375–382.

Mottonen, J., Strand, A., Symersky, J., Sweet, R. M., Danley, D. E., Geoghegan, K. F., Gerard, R. D., & Goldsmith, E. J. (1992) *Nature 355*, 270–273.

Nordenman, B., & Björk, I. (1987) *Biochemistry 17*, 3339–3344.

Olsen, S. T., & Björk, I. (1991) *J. Biol. Chem. 266*, 6353–6364.

Olsen, S. T., Srinivasan, K. R., Björk, I., & Shore, J. D. (1981) *J. Biol. Chem. 256*, 11073–11079.

Olsen, S. T., Halvorson, H. R., & Björk, I. (1991) *J. Biol. Chem. 266*, 6342–6352.

Oosta, G. M., Gardner, W. T., Beeler, D. L., & Rosenberg, R. D. (1981) *Proc. Natl. Acad. Sci. U.S.A. 78*, 833–839.

Oshima, G., & Nagasawa, K. (1986) *Thromb. Res. 37*, 361–372.

Owen, M. C., Borg, J.-Y., Soria, C., Soria, J., Caen, J., & Carrell, R. W. (1987) *Blood 69*, 1275–1279.
Petersen, L. C., & Jørgensen, M. (1983) *Biochem. J. 211*, 91–97.
Peterson, C. B., & Blackburn, M. N. (1987) *J. Biol. Chem. 262*, 7559–7566.
Peterson, C. B., Noyes, C. M., Pecon, J. M., Church, F. C., & Blackburn, M. N. (1987) *J. Biol. Chem. 262*, 8061–8065.
Pomerantz, M. W., & Owen, W. G. (1978) *Biochim. Biophys. Acta 535*, 66–77.
Schulze, A. J., Baumann, U., Knof, S., Jaeger, E., Huber, R., & Laurell, C.-B. (1990) *Eur. J. Biochem. 194*, 51–56.
Schulze, A. J., Frohnert, P. W., Engh, R. A., & Huber, R. (1992) *Biochemistry 31*, 7560–7565.
Skriver, K., Wikoff, W. R., Paston, P. A., Tausk, F., Schapira, M., Kaplan, A. P., & Bock, S. C. (1991) *J. Biol. Chem. 266*, 9216–9221.
Stein, P. E., Leslie, A. G. W., Finch, J. T., Turnell, W. G., McLaughlin, P. J., & Carrell, R. W. (1990) *Nature 347*, 99–102.
Stone, A. L., Beeler, D., Oosta, G., & Rosenberg, R. D. (1982) *Proc. Natl. Acad. Sci. U.S.A. 79*, 7190–7194.
Torri, G., Casu, B., Gatti, G., Petitou, M., Choay, J., Jacquinet, J. C., & Sinay, P. (1985) *Biochem. Biophys. Res. Commun. 128*, 134–140.
Tollefsen, D. M., Peacock, M. E., & Monafo, W. J. (1986) *J. Biol. Chem. 261*, 8854–8858.
Walker, A. C., & Schmidt, C. L. A. (1944) *Arch. Biochem. 5*, 445–467.
Wharton, C. W., & Szawelski, R. J. (1982) *Biochem. J. 203*, 351–360.
Whinna, H. C., Blinder, M. A., Szewczyk, M., Tollefsen, D. M., & Church, F. C. (1991) *J. Biol. Chem. 266*, 8129–8135.